

## ENERGY DEPENDENCE OF CROSS SECTIONS FOR $(n, \gamma)$ REACTIONS ON A NUMBER OF ODD-Z NUCLEI

Yu. P. POPOV and F. L. SHAPIRO

P. N. Lebedev Physics Institute, Academy of Sciences, U.S.S.R.

Submitted to JETP editor November 23, 1961

J. Exptl. Theoret. Phys. (U.S.S.R.) **42**, 988-1000 (April, 1962)

Curves are presented giving the energy dependence of the cross sections for radiative capture of neutrons with energies below 40 keV for Br, Rb, Nb, Rh, In, Sb, I, Cs, Ir and the enriched Rb<sup>85</sup> isotope. These were obtained with a spectrometer which measures the slowing down time in lead. Resonances not previously known were found in both of the Rb isotopes. The cross section data are compared with the results of other authors. The variation of the capture cross section averaged over resonances, as a function of number of nucleons in the nucleus, shows a clear effect of neutron shells and of the proton shell at  $Z = 50$ .

### INTRODUCTION

THE measurement of the energy dependence of the cross sections for radiative capture of neutrons by different nuclei is of great interest for nuclear theory, for the theory of the origin and distribution of the elements in nature, as well as from the point of view of construction of nuclear reactors (especially fast reactors) and the design of radiation shielding.

Such measurements in the 1–100 keV energy range have been begun only recently. The selection of neutrons of a definite energy is accomplished either by neutron time-of-flight with recording of the prompt gammas with a large-volume liquid scintillator,<sup>[1]</sup> or by using monoenergetic neutrons of controllable energy, obtained from a Van de Graaff using the  $\text{Li}^7(p, n)$  or  $\text{H}^3(p, n)$  reaction. In the latter case, the act of capture is recorded by observing the prompt  $\gamma$  rays<sup>[2]</sup> or by activation of a sample.<sup>[3-7]</sup>

As a rule, these methods permit one to obtain relative values of the capture cross section, which are then normalized to the absolute measurements made for one of the elements at a fixed neutron energy. However, in the kilovolt range absolute cross section measurements are complicated and the results obtained by different authors are often far outside their experimental errors. This discrepancy is especially apparent in the repeatedly measured neutron capture cross sections of silver, iodine and gold.<sup>[8,6]</sup>

The present measurements were made with a neutron spectrometer which uses the time of slowing down in lead;<sup>[9]</sup> in its present form this instru-

ment can measure capture cross sections from fractions of an eV up to 40–50 keV. Special attention was paid to the normalization of the cross section.

The study of the energy dependence of total neutron cross sections over the resonance region made possible the determination of the s-wave neutron strength function ( $S_0$ ) for a wide class of nuclei,<sup>[10]</sup> and led to further development and improvement of the optical model.<sup>[13-15]</sup> The determination of the p-wave neutron strength function ( $S_1$ ) is of interest, especially in the region of  $A \sim 100$ , where the optical model predicts the presence of a giant resonance in  $S_1$  as a function of  $A$ . Values of  $S_1$  can be obtained by analyzing the energy dependence of the averaged capture cross section for neutrons in the 1–100 keV energy region. These problems also motivated the present experiments.

Since the results of the measurements of the energy dependence of the neutron capture cross sections are of independent interest, they are published here before the completion of the computation of the strength functions for s and p neutrons.

### METHOD OF MEASUREMENTS\*

Briefly, the method of measurement of capture cross sections with the slowing-down spectrometer consists of the following. From the reaction  $\text{H}^3(d, n)\text{He}^4$  in a lead moderator (a cube), "neutron bursts" of 0.5–5  $\mu\text{sec}$  duration are produced. The average energy of the neutrons decreases as

\*The method is described in more detail in <sup>[16]</sup> (cf. also <sup>[17]</sup>).

they are slowed down, and is related to the slowing-down time by the formula:

$$\bar{E} = 183/(t + 0,3)^2, \quad (1)$$

where  $\bar{E}$  is in keV and  $t$  in microseconds.

A detector (scintillation counter or proportional gas-discharge counter) placed in a hole in the lead cube records  $\gamma$  rays alternately with and without a sample surrounding the detector. The delay time of the  $\gamma$  ray pulses in the detector relative to the neutron burst is analyzed in a multichannel analyzer.

For thin samples ( $\bar{n}\sigma \ll 1$ , where  $\bar{n}$  is the effective thickness, i.e., the number of nuclei per  $\text{cm}^2$ ), the effective cross section for capture of neutrons of energy  $\bar{E}(t)$  is computed from the expression

$$\sigma(n, \gamma) = k \frac{J_\gamma(t)}{J_B(t)} (t + 0,3). \quad (2)$$

Here  $J_\gamma(t)$  is the counting rate of prompt capture  $\gamma$  rays in the corresponding channel of the time analyzer, less background and a slight correction for activation of the sample and for capture of neutrons left over from the preceding cycle;  $J_B(t)$  is the counting rate in the same analyzer channel for a detector absorbing neutrons according to a  $1/v$  law (in particular, a boron counter<sup>[3, 17, 18]</sup>);  $k$  is a calibration factor which can be determined either from measurements in the thermal region or by measuring the area under a resonance (or group of resonances) with known parameters

$$k = \sum_i R_{\gamma i} / 2S_i, \quad (3)$$

where

$$R_\gamma = \frac{\pi\sigma_0\Gamma_\gamma}{2E_0}, \quad \text{and} \quad S = \int_{\text{res}} \frac{J_\gamma(t) dt}{J_B(t)}.$$

If the sample is thick,  $R_\gamma$  must be replaced by an effective resonance integral averaged over the neutron paths in the sample\*

$$R_{\gamma \text{ eff}} = \frac{\overline{A(n)}}{\bar{n}} \frac{\Gamma_\gamma}{\Gamma E_0}, \quad (4)$$

where

$$\overline{A(n)} = \int_{\text{res}} \frac{A(n)}{(1 - e^{-n\sigma})} dE. \quad (5)$$

In our case we set  $\overline{A(n)} = A(\bar{n})$ , which gives an error of no more than 3–5%. Graphs relating  $A(n)$  to the level parameters  $\sigma_0$  and  $\Gamma$  are given in the papers of Hughes and also Efimov and Shelontsev.<sup>[19]</sup> A correction has been made to

\*The sample is in the form of a cup or hollow cylinder (cf. <sup>[16]</sup>) and is irradiated by an isotropic neutron flux.

$A(\bar{n})$  for capture of the neutron after it has been once scattered resonantly.\*

The proposed method for normalizing the cross section assumes constant efficiency of the  $\gamma$ -ray detector over the whole range of variation of the neutron energy. A thick-wall proportional gas discharge counter<sup>[16, 20]</sup> satisfies this condition. Its efficiency for  $\gamma$  rays is proportional to the energy  $E_\gamma$ , and consequently its efficiency for recording neutron captures (with energy  $E \ll B$ ) is

$$\varepsilon = aB, \quad (6)$$

where  $B$  is the binding energy of the captured neutron in the nucleus, and  $a$  is a constant. Thus Eq. (2) is in principle valid for monoisotopic elements or for elements whose isotopes differ little in neutron binding energy.

As a check on our experiments, we also used a scintillation counter, for which (6) is not satisfied.<sup>[16]</sup> However, within the limits of accuracy of the measurements (see below), both detectors gave the same results for the elements presented here.

The determination of the calibration factor  $k$  from different resonances and groups of resonances with known parameters gave results agreeing within 5–10%. We used an averaged value of  $k$ . Normalization in the thermal region was not done, since the ratio of effect to background was much worse there than at resonance. On the other hand, the region where the ratio of effect to background is small is very sensitive to instabilities of operation of the equipment over the time of successive measurements of effect and background. Therefore, from the difference between  $\sigma_{\text{th}}$ <sup>[22]</sup> and the cross section in the thermal region when normalized at resonance, corrections were made in some cases for incorrect subtraction of background (especially for measurements with the scintillation counter). For the averaged cross sections, this correction was  $\lesssim 1\%$ .

When the element has no resonances with satisfactorily measured parameters and the thermal cross section is small (for example, for Rb), we used a normalization at resonances of other elements. For samples of identical dimensions,

$$k_x = k_{\text{st}} \frac{\alpha_{\text{st}} n_{\text{st}}^2 \varepsilon_{\text{st}}}{\alpha_x n_x \varepsilon_x}, \quad (7)$$

\*The correction was made using the formula  $\Delta A = T(w) \times (\Gamma_n/\Gamma)A(\bar{n})$ , where  $(\Gamma_n/\Gamma)A(\bar{n})$  is the number of neutrons which undergo resonance scattering,  $T(w)$  is the probability of interaction of a scattered neutron, as determined from Fig. 10 of <sup>[21]</sup>. For an isotropic neutron flux it is more correct to take  $w = 4E_0 m/M\sqrt{\bar{n}\sigma_0\Gamma^2/2}$ .

where  $k_x$ ,  $\alpha_x$ ,  $\bar{n}_x$  and  $\epsilon_x$  are respectively the normalization factor, monitor count, effective thickness and efficiency of recording of a single capture for the sample under investigation;  $k_{st}$ ,  $\alpha_{st}$ ,  $\bar{n}_{st}$  and  $\epsilon_{st}$  are the same for the standard sample.

Since the simple dependence (6) does not hold for the scintillation counter, it is not possible in general to determine the ratio  $\epsilon_{st}/\epsilon_x$  in formula (7) and thus obtain a normalization of the cross section for one element in terms of another.

If the sample and standard differ in dimensions, corrections of a geometrical nature enter in (7). These corrections were made experimentally.

To estimate the effect of self-shielding, measurements were made with different sample thicknesses for each element. These measurements showed (see below) that for  $E > 2$  keV the effect of self-shielding is absent (to an accuracy of 3–5%) for all the samples ( $\bar{n} < 5 \times 10^{21}$  cm $^{-2}$ ), and the experimental points give the true cross sections averaged over many resonances.

Corrections of up to 5% were made for counting errors caused by the heavy loading immediately following the neutron burst.

We considered the following effects, which in principle may affect the results of the measurements: a) absorption of  $\gamma$  ray background in the sample; b) errors in determining the  $\gamma$  ray background due to distortion of the neutron spectrum by the sample;<sup>[16]</sup> c) poor resolution of the spectrometer in the high energy region;\* d) in the case of substances with two isotopes (Br, Rb, In, Sb, Ir), the difference in binding energy of the isotopes, which results in differences in efficiency of recording neutron captures; e) the effect of elastic scattering of neutrons by the materials in the detector on the resonance capture in the sample.

Corrections for these effects were not made.

Scattering of neutrons by detector materials gives rise to two effects, depending on geometrical conditions and on the characteristics of the resonance: a) the absorbing sample screens the scatterer, which results in a reduction of the neutron flux which is incident from the side of the scatterer facing the sample; b) the scatterer (moderator) which is inside the sample reduces the screening of some parts of the sample from other parts. The first effect reaches its maximum value when the

\*Expression (2) can be written in the form  $J_\gamma(t)/J_B(t) = k_1 \langle \sigma_\gamma v \rangle = k_1 \sigma_\gamma(\bar{E})v(\bar{E})(1 + \delta)$ , where  $\langle \rangle$  denotes an average over the neutron spectrum at time  $t$ ,  $\delta$  is a correction for the finite resolution of the spectrometer. If  $\sigma_\gamma v \sim E^{-p}$ , then for this spectrometer  $\delta \approx \frac{1}{2}p(p+1)\bar{E}_{keV}\%$ . For  $\sigma \sim E^{-1/2}$ ,  $\delta = 0$ ; for  $\sigma \sim E^{-3/4}$  and  $E = 30$  keV,  $\delta = 5\%$ .

effective width of the absorption band is  $\Gamma_{eff} > 4E_0/A$ ; it reduces the resonance absorption. The second effect may be significant for  $\Gamma_{eff} \ll 4E_0/A$  and increases the resonance absorption. For some elements the calibration factor  $k$  was found from resonance levels satisfying one or the other condition; for all elements the measurements were done with several sample thicknesses and with two detectors having markedly different geometrical characteristics and slowing-down power. For  $E > 2-3$  keV, no systematic differences were observed in the measured cross sections. For this reason we assume that scattering of neutrons by the materials of the detector played no important role in the measurements.

The errors which may be introduced by effects a, b, c and d were evaluated experimentally or by computation, and it was shown that each of them cannot exceed 1–3%. Together with the error in absolute normalization of the cross section and the statistical error ( $\sim 1-3\%$ ) they gave the main contribution to the overall error of the measurements, which did not exceed 10% for  $E < 10$  keV and 15% for  $E > 10$  keV. Only in the low-energy region, between individual resonances, where the ratio of effect to background is small, does the error exceed 10%. The mean square error of the cross section, computed for some of the elements from the spread in measurements made with different samples and detectors, amounts to  $\sim 3\%$  for  $E = 10$  keV.

## RESULTS OF MEASUREMENTS

For all of the elements, the measurements of the neutron capture cross section were made for several sample thicknesses. Figures 1–9 show the cross section curves, usually for the thickest and thinnest samples.

Bromine (Fig. 1). The measurements were made on samples of AlBr $_3$  and KBrO $_3$ . For  $E < 10$  keV, the cross section follows the  $1/v$  law and coincides with the measurements in the thermal region.<sup>[22]</sup> For  $E > 10$  keV, our measurements lie 30–50% below the data of Gibbons et al, which are given in<sup>[8]</sup>. In the published data of the same authors,<sup>[1]</sup> only the reference points at 30 and 65 keV are given, and the cross sections are reduced, so that they agree better with our results.

Rubidium (Fig. 2). The dashed curve is the cross section for Rb $^{85}$  (10.8 g of Rb $_2$ SO $_4$  with 98.8% enrichment), while the solid curve is the cross section for the normal mixture of isotopes (where we used RbNO $_3$  marked “pure” from Czechoslovakia and Rb $_2$ SO $_4$  obtained from Soviet-produced RbCl marked “pure”).

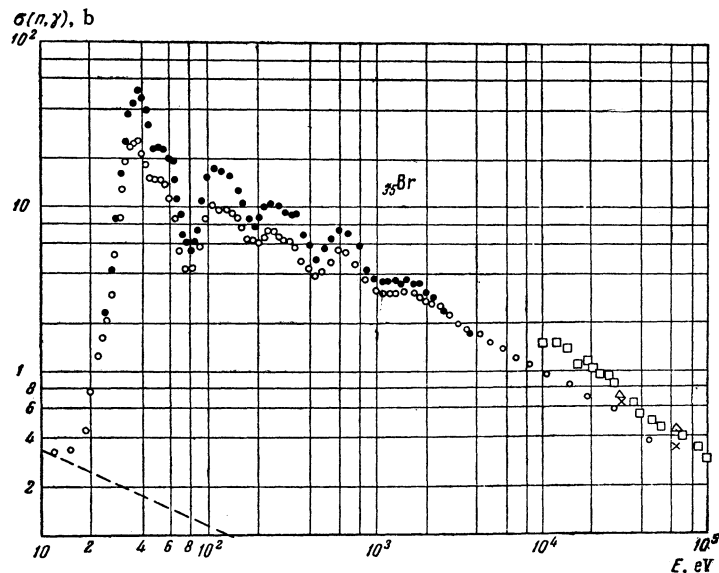


FIG. 1. Energy dependence of neutron capture cross section of bromine. The dotted line is the cross section extrapolated according to the  $1/v$  law from the thermal region;  $\bullet$ — $\bar{n} = 2.2 \times 10^{21}$  nuclei/cm<sup>2</sup>,  $\circ$ — $\bar{n} = 7.5 \times 10^{21}$  nuclei/cm<sup>2</sup>;  $\square$ ,  $\Delta$ —data of Gibbons et al,<sup>[8]</sup>  $\times$ —data of [1].

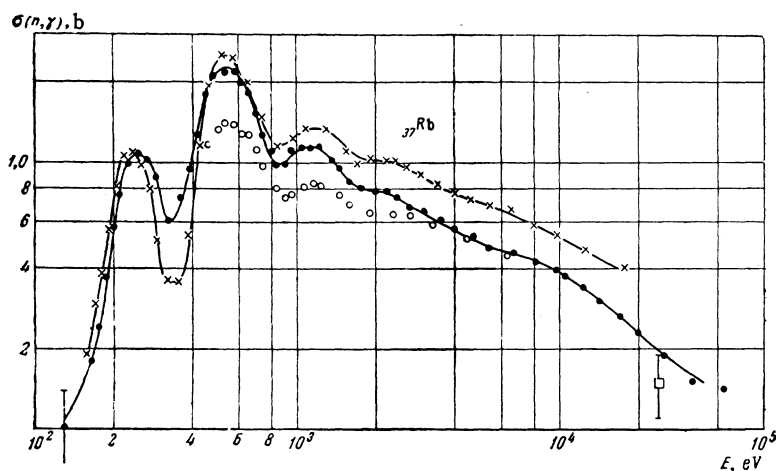


FIG. 2. Energy dependence of neutron capture cross section by nuclei of normal rubidium ( $\bullet$ — $\bar{n} = 4.0 \times 10^{21}$  nuclei/cm<sup>2</sup>,  $\circ$ — $\bar{n} = 16 \times 10^{21}$  nuclei/cm<sup>2</sup>) and the  $\text{Rb}^{85}$  isotope ( $\times$ — $\bar{n} = 3.5 \times 10^{21}$  nuclei/cm<sup>2</sup>);  $\square$ —data of [23].

Because rubidium has no resonances with known parameters for  $E < 1$  keV,<sup>[8]</sup> and since the thermal cross section is small, the cross section curves were normalized in terms of other elements. The measurements with the proportional counter as detector were calibrated in terms of Br and  $\text{Mo}^{95}$  resonances, while those with the scintillation counter were calibrated using Br and the thermal cross section of Cl. In the energy region  $E > 3$  keV, where the sample thickness no longer affects the results, the curves for all three series of measurements coincided within 5–10%.

Such an agreement of the normalizations for the case of the normal mixture of rubidium isotopes using proportional and scintillation counters gives us confidence in the normalization of the measurements on  $\text{Rb}^{85}$ , for which only the scintillation counter was used.

In the energy region below 100 eV, which is not shown in Fig. 2, the accuracy of the cross section determination was low, but for all samples including the enriched ones a weak resonance appeared

at  $\sim 9.3$  eV, for which the parameters could not be measured. In order to estimate the contribution of the  $\text{Rb}^{87}$  isotope to the cross section of the normal mixture of rubidium isotopes ( $\text{Rb}^{85}$ —72.15%,  $\text{Rb}^{87}$ —27.85%), the cross section curve for  $\text{Rb}^{85}$  was computed per atom of the normal mixture and subtracted from the solid curve of Fig. 2.

As a result we found that in addition to the resonances of  $\text{Rb}^{85}$  at  $E_0 = 230$  eV and the group of unresolved resonances with  $E_0 \sim 500$ –700 eV, there are resonances of  $\text{Rb}^{87}$  with  $E_0 \sim 280$  and 410 eV. For  $E > 2$  keV, the calculated cross section of  $\text{Rb}^{85}$  and the cross section for the normal mixture coincide within the limits of accuracy of the measurement ( $\sim 10\%$ ), so that the contribution of  $\text{Rb}^{87}$  is  $\lesssim 15\%$  of the capture cross section of the element. Such a value at  $E = 24$  keV does not contradict the results of activation measurements with antimony-beryllium neutrons ( $75 \pm 15$  mb<sup>[23]</sup> and  $29 \pm 1.4$  mb<sup>[24]</sup> per atom of  $\text{Rb}^{87}$ ). The parameters of the new levels were found by the method described in<sup>[16]</sup>, and are shown in the table (where

$E_0$ , eV	Isotope	$\sigma_0\Gamma$ , b-eV	$10^3\Gamma_n$ , eV	$\Gamma_\gamma$ , eV
9.3	(Rb <sup>85</sup> )	—	—	—
230 $\pm$ 15	Rb <sup>85</sup>	93 $\pm$ 10	17 $\pm$ 2	0.44 $\pm$ 0.15
280 $\pm$ 20	Rb <sup>87</sup>	100 $\pm$ 30	22 $\pm$ 7	0.250 <sup>[8]</sup>
410 $\pm$ 30	Rb <sup>87</sup>	85 $\pm$ 20	40 $\pm$ 16	0.250 <sup>[8]</sup>
500—700	mainly Rb <sup>85</sup>	a group of unresolved levels		

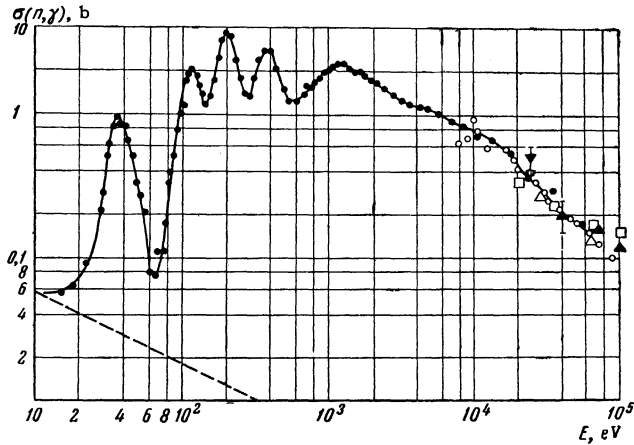


FIG. 3. Energy dependence of neutron cross section of niobium. The dashed curve is the cross section extrapolated according to the  $1/v$  law from the thermal region;  $\bullet$  —  $\bar{n} = 4.6 \times 10^{21}$  nuclei/cm<sup>2</sup>;  $\Delta$ ,  $\circ$  — data of [1],  $\square$  — data of [2],  $\blacktriangle$  — [5],  $\nabla$  — [25].

we assume that the statistical factor is  $g = 1/2$ ).

**Niobium** (Fig. 3). The measurements were made on pure samples of metallic Nb and Nb<sub>2</sub>O<sub>5</sub> of various thicknesses. The calibration coefficients were determined from the four groups of levels with  $\bar{E} \sim 36, 120, 200$  and  $380$  eV, [8] and coincided within 8–10%. For  $E > 10$  keV, the cross section behavior agrees well with the data of other authors. [1,2,5,25]

**Rhodium** (Fig. 4). Preliminary data on rhodium

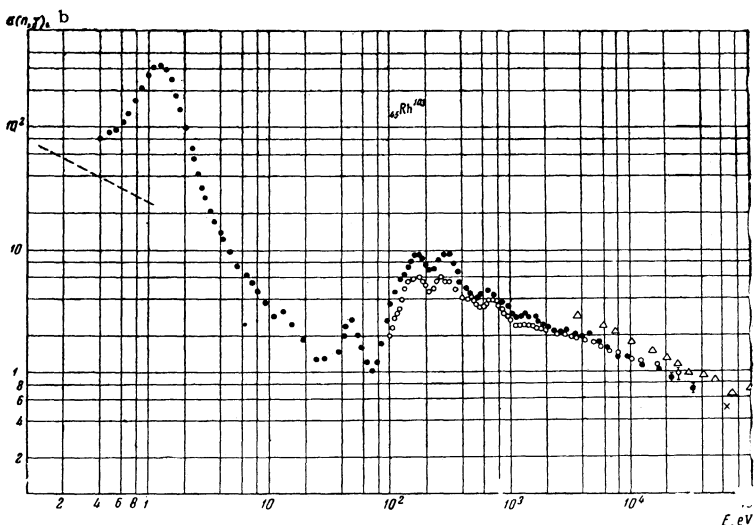


FIG. 4. Energy dependence of neutron capture cross section of rhodium:  $\bullet$  —  $\bar{n} = 2.2 \times 10^{21}$  nuclei/cm<sup>2</sup>,  $\circ$  —  $\bar{n} = 4.7 \times 10^{21}$  nuclei/cm<sup>2</sup>,  $\times$  — data of [1],  $\Delta$  — [4].

were reported at the Tashkent conference in 1959 [26] (the curve for  $n = 4.7 \times 10^{21}$  nuclei/cm<sup>2</sup>). Calibration coefficients computed from the parameters of the resonances at  $E_0 = 1.257$  eV, and  $\bar{E} \sim 45$  and  $160$  eV, agree within 7–10%.

Our results are 30% lower than the cross sections measured by Weston et al. [4]. The similarity of our results and theirs indicates that the difference is probably caused by an incorrect normalization of the cross section curve. In that case the results of Gibbons et al. [1] at  $E = 65$  keV favor our data.

**Indium** (Fig. 5). The measurements were made with indium foils of various thicknesses. The results were normalized at four groups of levels; three of them gave calibration coefficients  $k$  which coincided within 3% (for  $\bar{E} < 6.5$  eV,  $\bar{E} \sim 10$  eV and  $\bar{E} \sim 40$  eV), while in all the measurements the fourth group ( $E \sim 24$  eV) gave a value of  $k$  about 10% lower than the others. It would be desirable to make a more careful measurement of the parameters of the indium levels at  $E_0 = 21.6, 23$  and  $25.2$  eV, which are included in this group.

For  $E > 25$  keV our results are in good agreement with other data [1,4,27] and in somewhat poorer agreement with activation measurements with Sb-Be neutrons. [23,28] Below 25 keV our data lie between the points obtained in [1] and [4], which differed by 50–70%.

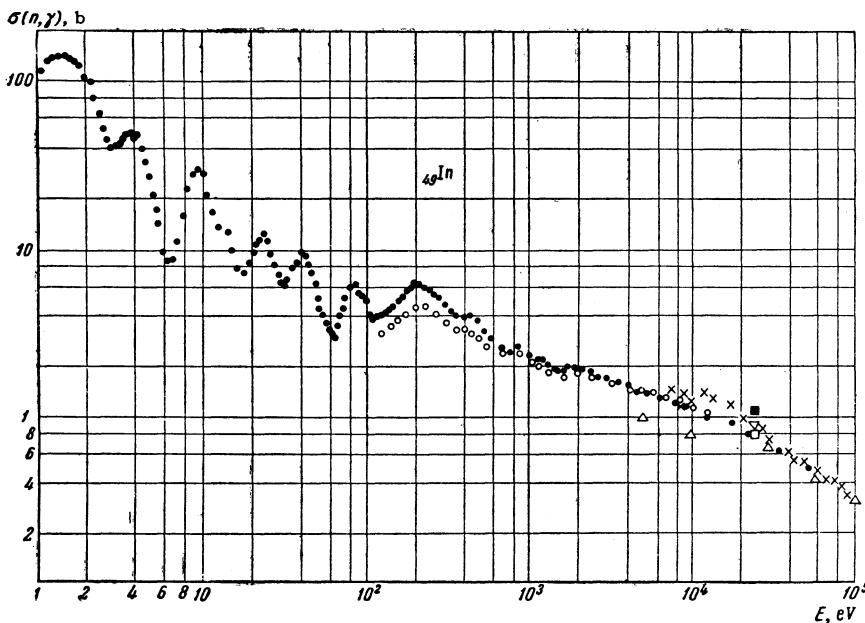


FIG. 5. Energy dependence of neutron capture cross section of indium;  $\bullet$ — $\bar{n} = 5.8 \times 10^{21}$  nuclei/cm<sup>2</sup>,  $\circ$ — $\bar{n} = 12.6 \times 10^{21}$  nuclei/cm<sup>2</sup>,  $\times$ —data of [1],  $\square$ —[27],  $\Delta$ —[4],  $\nabla$ —[23],  $\blacksquare$ —[28]. The last three papers measured the cross section for activation of  $\text{In}^{115}$ , so we give the value of  $\sigma[\text{In}^{115}(54 \text{ min})] \times 1.15$ .

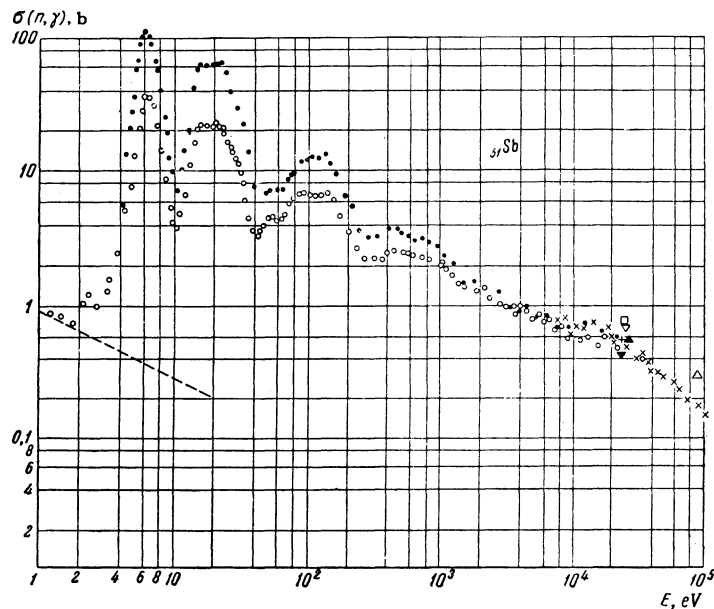


FIG. 6. Energy dependence of neutron capture cross section of antimony. The dashed curve is the cross section extrapolated to a  $1/v$  law from the thermal region;  $\bullet$ — $\bar{n} = 0.56 \times 10^{21}$  nuclei/cm<sup>2</sup>,  $\circ$ — $\bar{n} = 5.6 \times 10^{21}$  nuclei/cm<sup>2</sup>,  $\times$ —data of [1],  $\square$ —cited in [8],  $\nabla$ —[23],  $\blacktriangledown$ —[25],  $+$ —[27],  $\blacktriangle$ —[28],  $\triangle$ —[29].

**Antimony** (Fig. 6). The samples were prepared from metallic antimony, mark STs-0 (99.85% Sb). The cross section was normalized using the parameters of the level at  $E_0 = 6.24$  eV and the group of levels around  $\bar{E} \sim 17$  eV.<sup>[8]</sup> Measurements with thick and thin samples at  $E \sim 15$  keV gave results differing by 15–20%. The origin of this discrepancy is not clear.

For the thin sample, our data agree with the cross section behavior in [1] and the measurements at  $E = 24$  keV,<sup>[25,27,28]</sup> but they run somewhat lower than the data of [23] and the unpublished results from Berkeley, which are given in [8].

**Iodine** (Fig. 7). The samples were made of "pure" quality elementary iodine. The cross section was normalized to the parameters of two

groups of levels<sup>[8]</sup> (31.4–46.3 eV and 66.3–91 eV), which gave the same calibration factor within 2.3%. Our results are in good agreement with the data of [1,4,23,25] but our somewhat lower than those of [7,30].

**Cesium** (Fig. 8). Measurements were made with cesium carbonate samples of various thicknesses. The cross section was normalized to the parameters of the three lowest levels and to the group of levels at  $\bar{E} \sim 100$  eV;<sup>[8]</sup> the calibration factors were the same to within 5–8%.

The only data on capture in cesium with which one can compare our results are those for activation of Cs using an antimony-beryllium source.<sup>[28]</sup> Those results are  $\sim 50\%$  higher than ours.

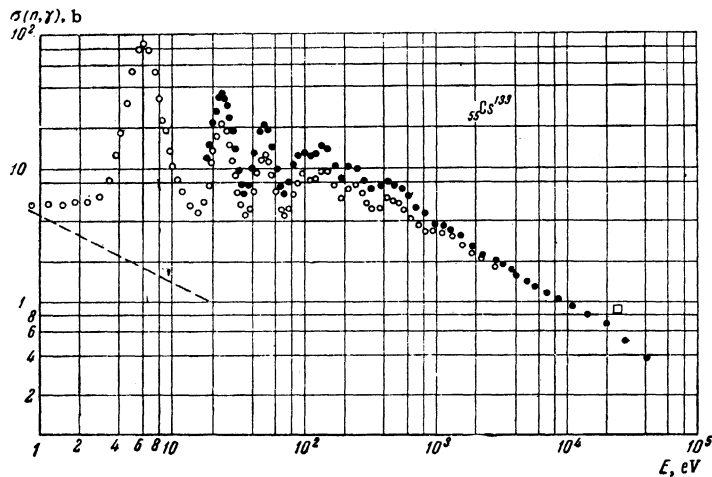


FIG. 8. Energy dependence of neutron capture cross section of cesium. The dashed curve is the cross section extrapolated according to the  $1/v$  law from the thermal region;  $\bullet - \bar{n} = 1.3 \times 10^{21}$  nuclei/cm<sup>2</sup>,  $\circ - \bar{n} = 4.0 \times 10^{21}$  nuclei/cm<sup>2</sup>,  $\square$  - data of [28].

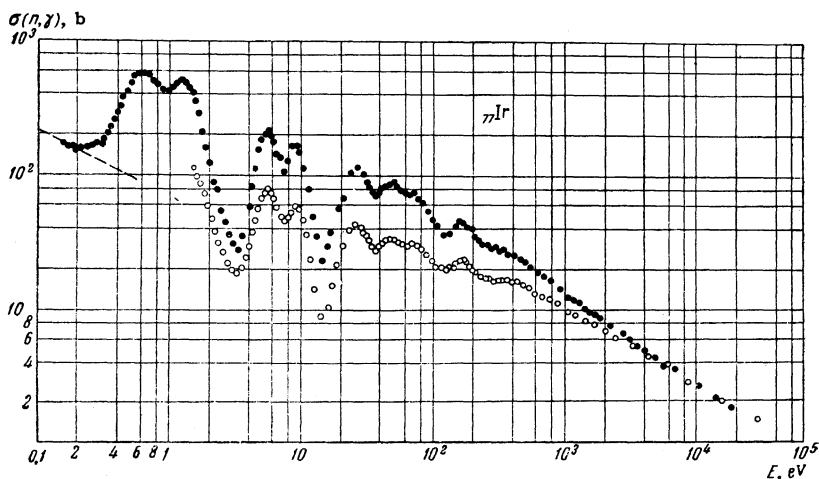


FIG. 9. Energy dependence of neutron capture cross section of iridium. The dashed curve is the cross section extrapolated according to the  $1/v$  law from the thermal region;  $\bullet - \bar{n} = 0.7 \times 10^{21}$  nuclei/cm<sup>2</sup>,  $\circ - \bar{n} = 6.3 \times 10^{21}$  nuclei/cm<sup>2</sup>.

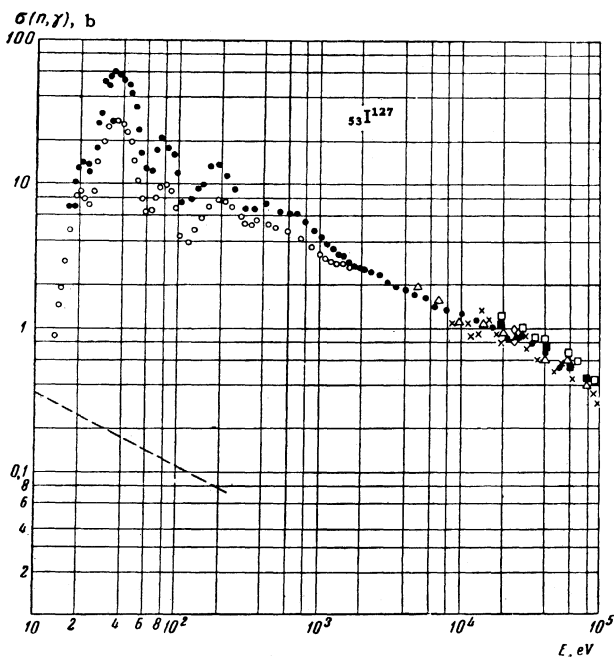


FIG. 7. Energy dependence of neutron capture cross section of iodine. The dashed curve is the cross section extrapolated according to a  $1/v$  law from the thermal region;  $\bullet - \bar{n} = 1.7 \times 10^{21}$  nuclei/cm<sup>2</sup>,  $\circ - \bar{n} = 6.6 \times 10^{21}$  nuclei/cm<sup>2</sup>,  $\times$  - data of [1],  $\Delta$  - [4],  $\blacksquare$  - [7],  $\nabla$  - [23],  $\blacktriangle$  - [27],  $\square$  - [30],  $\diamond$  - [35].

Iridium (Fig. 9). The measurements of the neutron capture cross section were made on samples of metallic iridium. Normalization of the cross section using the resonance parameters [8] and using the thermal cross section with a slight correction for self-shielding gave identical results.

No other data are available on neutron capture in iridium.

CONCLUSION

The results for neutron capture obtained with the slowing-down spectrometer are essentially in good agreement with the data of other authors at the same energies. This is shown very well in Fig. 10, for  $E = 30$  keV, where we give the dependence of the averaged neutron capture cross section on atomic number of the target nuclei for odd-Z nuclei. Figure 10 shows clearly the effect of closed neutron shells and the weaker effect of the closed proton shell at  $Z = 50$ . The curve retains the same appearance for lower neutron energies, down to 3 keV.\*

\*A similar dependence is given by Gibbons et al [1] for  $E = 65$  keV. Shell effects have also been seen at high neutron energies: 400 keV [31] and  $\sim 1$  MeV [32].

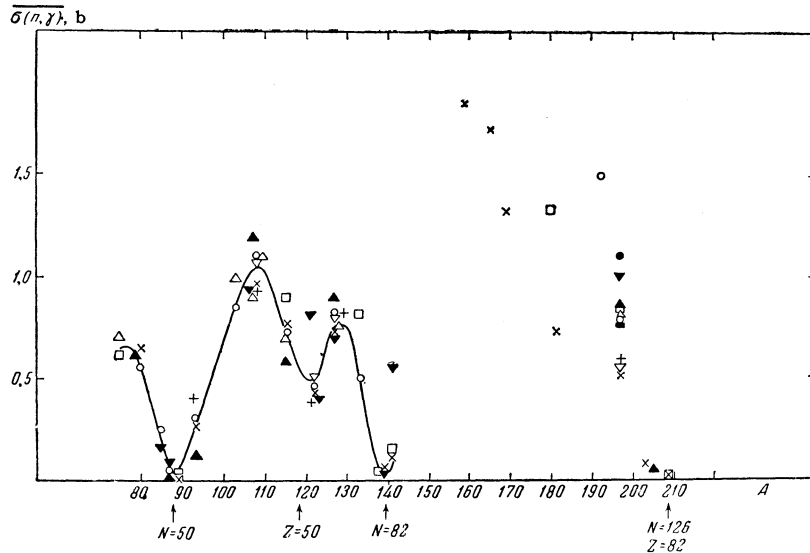


FIG. 10. Dependence of averaged radiative capture cross section of neutrons on mass number  $A$  of target nuclei, for odd  $Z$  ( $E = 30$  keV);  $\circ$ —data obtained with the Pb slowing-down spectrometer,  $\times$ —data of [1],  $\Delta$ —[3,4],  $\bullet$ —[6],  $\nabla$ —[23],  $\nabla$ —[27],  $\square$ —[28],  $+$ —[25],  $\blacktriangle$ —[24,30],  $\blacksquare$ —[36]. The results of measurements with an antimony-beryllium source ( $E = 24$  keV), when extrapolated to  $E = 30$  keV, gave a curve parallel to the measured curve. The point  $\circ$  for  $\text{Rb}^{87}$  is the upper limit of the cross section ( $\sim 0.05$  barn) obtained in our measurements.

In our measurements with Rb, a large number of resonances with  $E_0 < 2$  keV were seen which have not been seen in total cross section measurements.<sup>[8,33]</sup> In the region  $E > 2$  keV, the known resonances account for only  $1/4$ — $1/8$  of the averaged capture cross section, depending on one's assumption for the value of the radiation width (in our measurements on the  $\text{Rb}^{85}$  resonance at  $E_0 = 230$  eV, we obtained a value of  $\Gamma_\gamma$  which is twice as great as that used in [8], which was an average of the measurements on neighboring elements). Thus we see that the authors of [33] obtained too high values of the level spacing in  $\text{Rb}^{85}$  and  $\text{Rb}^{87}$  ( $1 \pm 0.5$  keV and  $2 \pm 1$  keV, respectively).

The measurements show that despite some definite faults—poor resolution of the spectrometer\* and limitation on the high energy side—the slowing-down spectrometer has the following advantages over other methods.

1. One can measure the neutron capture cross section in the region below 5—10 keV, which is difficult to reach with other spectrometers.

2. One can get a satisfactory normalization of the cross section using the parameters of low-lying resonances, which are well known, or one can normalize to the cross section in the thermal region.

3. It makes possible measurements with thin samples ( $\bar{n} \leq 10^{21}$  nuclei/cm<sup>2</sup>), with a total sample weight of a few grams (the thin sample of Ir was 0.3 g). A lower limit is imposed on the cross section which can be measured because of the background of  $\gamma$  rays from capture in the lead, and is approximately

\*The full width of an individual resonance at half maximum is constant for  $E \leq 1$  keV and  $\sim 35\%$ , while it grows for larger energies, reaching  $\sim 70\%$  at  $E = 15$  keV.<sup>[64]</sup>

$$\sigma_\gamma > 0.2E^{-1/2} \text{ barn for } E < 1 \text{ keV,}$$

$$\sigma_\gamma > E^{-1/2} \text{ barn for } E > 1 \text{ keV}$$

where  $E$  is the neutron energy in eV.

4. In addition to measurements of averaged cross sections, the slowing-down method is also applicable to detecting negative levels,<sup>[16,26]</sup> measuring resonance absorption integrals, and analysis of materials for impurities which have strong isolated resonances (for example, Ag, Co, Mn, Cu and others). Effective resonance integrals can be measured for sample thicknesses up to a few millimeters; the limitation on thickness is related to the absorption of capture  $\gamma$  rays in the sample.

5. The method gives high luminosity; the measuring equipment is relatively cheap and simple.

In conclusion the authors express their gratitude to V. Ivanov, M. Ivanov, Irzhi Kvitek, A. Mokrushin, S. Romanov and É. Rudak for participating in the measurements on individual elements, and to Yu. A. Dmitrenko, S. N. Gubernov, A. M. Klabukov and E. D. Bulatov, who kept the equipment operating. The authors are grateful to V. S. Zolotarev and his coworkers, who prepared the samples containing separated isotopes.

<sup>1</sup>Gibbons, Macklin, Miller, and Neiler, Phys. Rev. **122**, 182 (1961).

<sup>2</sup>Yu. Ya. Stavisskiĭ and A. V. Shapar', Atomnaya Énergiya **10**, 264 (1961).

<sup>3</sup>Bilpuch, Weston, and Newson, Ann. Phys. **10**, 455 (1960).

<sup>4</sup>Weston, Seth, Bilpuch, and Newson, Ann. Phys. **10**, 477 (1960).

<sup>5</sup>Yu. Ya. Stavisskiĭ and V. A. Tolstikov, Atomnaya Énergiya **9**, 401 (1960).

<sup>6</sup>S. A. Cox, Phys. Rev. **122**, 1280 (1961).



- <sup>7</sup> S. J. Bame and R. L. Cubitt, *Phys. Rev.* **113**, 256 (1959).
- <sup>8</sup> Hughes, Magurno, and Brussel, *Neutron Cross Sections*, Suppl. N1 to BNL-325, 2nd ed., 1960.
- <sup>9</sup> Lazareva, Feinberg, and Shapiro, *JETP* **29**, 381 (1955), *Soviet Phys. JETP* **2**, 351 (1956). Bergman et al., *Proc. Geneva Conference*, 1955, vol. 4, p. 766. Bergman, Isakov, Popov, and Shapiro in *Yadernye reaktsii pri nizkikh i srednikh énergiyakh (Nuclear Reactions at Low and Medium Energies)* Moscow, 1958, p. 140.
- <sup>10</sup> *Nuclear Data Tables*, U. S. Government Printing Office, 1959.
- <sup>11</sup> Feshbach, Porter, and Weisskopf, *Phys. Rev.* **96**, 448 (1954).
- <sup>12</sup> P. E. Nemirovskii, *Sovremennye modeli atomnogo yadra (Contemporary Models of the Nucleus)* Atomizdat, 1960.
- <sup>13</sup> V. V. Vladimirskii and I. L. Il'ina, in *Nuclear Reactions at Low and Medium Energies*, Moscow, 1958, p. 124.
- <sup>14</sup> B. Margolis and E. S. Troubetskoy, *Phys. Rev.* **106**, 105 (1957).
- <sup>15</sup> Chase, Wilets, and Edmonds, *Phys. Rev.* **110**, 1080 (1958).
- <sup>16</sup> Kashchukeev, Popov, and Shapiro in *Neitronnaya Fizika (Neutron Physics)*, ed. Krupchitskii, Atomizdat, 1961, p. 354; *J. Nuclear Energy* **A14**, 76 (1961).
- <sup>17</sup> A. A. Bergman and F. L. Shapiro, *JETP* **40**, 1270 (1961), *Soviet Phys. JETP* **13**, 895 (1961).
- <sup>18</sup> H. Bichsel and T. W. Bonner, *Phys. Rev.* **108**, 1025 (1957). Bergman, Isakov, Popov and Shapiro, in *Nuclear Reactions at Low and Medium Energies*, Moscow, 1958, p. 17.
- <sup>19</sup> D. J. Hughes, *J. Nuclear Energy* **1**, 237 (1955). V. N. Éfimov and Yu. I. Shelontsev, Preprint R-641, Joint Inst. Nucl. Res., 1961.
- <sup>20</sup> A. I. Okorokov, Diploma thesis, Physics Institute, Academy of Sciences, 1958.
- <sup>21</sup> E. Melkonian, *Proc. Geneva Conference*, 1955, vol. 4, p. 340.
- <sup>22</sup> D. J. Hughes and R. B. Schwartz, *Neutron Cross Sections*, BNL-325, 2nd ed., 1958.
- <sup>23</sup> Macklin, Lazar and Lyon, *Phys. Rev.* **107**, 504 (1957).
- <sup>24</sup> Kononov, Stavisskii, and Tolstikov, *Atomnaya Énergiya* **5**, 564 (1958).
- <sup>25</sup> T. S. Balanova, Dissertation, Physics Institute, Academy of Sciences, Ukr. S.S.R., 1960.
- <sup>26</sup> Isakov, Popov, and Shapiro, *Reports of the Tashkent Conference on Peaceful Uses of Atomic Energy*, 1959; Tashkent, 1961, p. 64.
- <sup>27</sup> H. W. Schmitt and C. W. Cook, *Nuclear Phys.* **20**, 202 (1960).
- <sup>28</sup> Booth, Ball and McGregor, *Phys. Rev.* **112**, 226 (1958).
- <sup>29</sup> J. H. E. Griffiths, *Proc. Roy. Soc. (London)* **A170**, 513 (1939).
- <sup>30</sup> Yu. Ya. Stavisskii and V. A. Tolstikov, *Atomnaya Énergiya* **10**, 158 (1961).
- <sup>31</sup> Diven, Terrell, and Hemmendinger, *Phys. Rev.* **120**, 556 (1960).
- <sup>32</sup> D. J. Hughes and D. Sherman, *Phys. Rev.* **78**, 632 (1960).
- <sup>33</sup> Newson et al., *Ann. Phys.* **14**, 346 (1961).
- <sup>34</sup> Yu. P. Popov and F. L. Shapiro, *JETP* **40**, 1610 (1961), *Soviet Phys. JETP* **13**, 1132 (1961).
- <sup>35</sup> T. S. Belanova, *Atomnaya Énergiya* **8**, 549 (1960).
- <sup>36</sup> L. W. Weston and W. S. Lyon, *Phys. Rev.* **123**, 948 (1961).